

Enhanced thermal Hall conductivity below 1 Kelvin in the pyrochlore magnet $\text{Yb}_2\text{Ti}_2\text{O}_7$

Max Hirschberger,^{1,*} Peter Czajka,¹ S. M. Koohpayeh,² Wudi Wang,¹ N. Phuan Ong¹

¹*Department of Physics, Princeton University, Princeton NJ 08540 USA*

²*Institute for Quantum Matter, Department of Physics & Astronomy,
Johns Hopkins University, Baltimore MD 21218 USA*

(Dated: July 30, 2019)

Abstract

In this letter, we report the gigantic thermal Hall effect κ_{xy} in the low-field correlated-paramagnetic state of the frustrated pyrochlore $\text{Yb}_2\text{Ti}_2\text{O}_7$. We observed a record magnitude for the thermal Hall angle in an insulator, $|\kappa_{xy}|/\kappa_{xx} \sim 2\%$. The signal onsets at $T \sim 3\text{K}$ and is severely weakened around the transition to canted ferromagnetic order at $T_{\text{CFM}} = 0.275\text{K}$. Besides the large $\kappa_{xy} > 0$ of the fluctuating regime, a sign change towards negative κ_{xy} occurs at the lowest temperatures and in moderate field, where sharp magnon excitations appear in the inelastic neutron scattering spectra. We analyze the magnon-Hall signal and its suppression with field semi-quantitatively. A contribution of phonon skew scattering to κ_{xy} is ruled out by a comparison of κ_{xx} for Tb-, Yb-, and Y-based rare earth pyrochlore titanates. These results represent the first report of non-vanishing κ_{xy} measured in a dilution refrigerator ($T < 0.29\text{K}$).

When a condensed matter system is slightly nudged out of equilibrium by an applied heat current $J_{Q,i}$, quasiparticles such as electrons, magnetic excitations, and phonons drift along the resulting temperature gradient $\partial_i T$. The thermal transport tensor is defined as the linear response function relating these two quantities viz. $J_{Q,i} = \kappa_{ij} \partial_j T$ ¹. Broken time-reversal symmetry, e.g. through spontaneous ordering or an externally applied magnetic field H^2 , in principle allows for off-diagonal components of κ_{ij} : This is the thermal Hall or Righi-Leduc effect. Specializing to the case of insulators, $\kappa_{xy} \neq 0$, i.e. a transverse (Lorentz) force acting on charge-neutral quasiparticles, may seem surprising. Microscopic mechanisms for κ_{xy} in insulators have therefore been considered from a theoretical perspective only over the past fifteen years³⁴⁵⁶.

In the absence of a classical Lorentz force, it is believed that an important and likely dominant contribution to κ_{xy} in systems with non-interacting quasiparticles can be written as⁴⁶

$$\kappa_{xy} = - (k_B^2 T) / V \sum_{n\mathbf{k}} \Omega_{n\mathbf{k}}^z c_2(\rho_B(\epsilon_{n\mathbf{k}})) \quad (1)$$

where the summation is executed over all quasiparticle bands $\epsilon_{n\mathbf{k}}$ with momentum \mathbf{k} and band index n . $\Omega_{n\mathbf{k}}^z$ is the component of the Berry curvature vector parallel to the magnetization vector, ρ_B is the appropriate distribution function (e.g. Bose-Einstein), and $c_2(\rho_B)$ is a nonlinear, but monotonically decreasing function⁶. Eq. 1 for κ_{xy} is explicitly independent of the mean free path of heat carriers, similar to the case of the intrinsic anomalous Hall conductivity in electron gases with non-trivial band structures⁷⁸.

Through Eq. 1, it has become possible to quantitatively calculate the thermal Hall response of ferromagnets both in the long-range ordered state and above T_C ⁹¹⁰¹¹. This approach makes low- T transport experiments powerful complements to spectroscopic techniques such as inelastic neutron scattering, particularly due to their sensitivity to the lowest lying excitations. In addition to a wealth of theoretical predictions of κ_{xy} in various non-ferromagnetic long-ranged ordered magnets, the focus of recent theoretical and experimental research has moved towards frustrated magnets and spin liquids, their exotic elementary excitations, and associated κ_{xy} ¹²¹³¹⁴¹⁵¹⁶. In this letter, we report on the gigantic κ_{xy} in the fluctuating regime of a frustrated magnet, with high sensitivity to H and the onset of long-range order at the lowest T . As previous work identified signatures of strongly interacting magnon states in the same region of the phase diagram where the Hall angle is large³²³⁷,

our experiment highlights the potential of strongly interacting or fractionalized excitations for generating gigantic κ_{xy} , possibly requiring a theoretical framework beyond Eq. 1.

Target Material. The frustrated pyrochlore titanate $\text{Yb}_2\text{Ti}_2\text{O}_7$ is a well-studied compound for which highly stoichiometric single crystals of excellent quality have recently been grown using a traveling-solvent float zoning technique¹⁷¹⁸. In the pyrochlore structure of corner-sharing tetrahedra, the crystal electric field (CEF) environment at the rare earth site (Fig. 1) results in a simple level scheme for the $^2F_{7/2}$ Yb^{3+} ion: the ground-state Kramers doublet is separated from all higher CEF states by an energy gap $\epsilon_1 > 800 \text{ K}^{19}$. Then, the full exchange Hamiltonian \mathcal{H}_{ex} is commonly expressed in terms of pseudospin-1/2 operators S_i^z and S_i^\pm defined with respect to the *local* Ising axis (Fig. 1 (b)).

As compared to the classical spin-ice systems $\text{Ho}_2\text{Ti}_2\text{O}_7$ and $\text{Dy}_2\text{Ti}_2\text{O}_7$ with very strong local-Ising anisotropy, with $\mathcal{H}_{ex} \approx \sum_{ij} J_{zz} S_i^z S_j^z$, and with macroscopic ground state degeneracy²⁰²¹²², fluctuations between up- and down-states are enhanced in $\text{Yb}_2\text{Ti}_2\text{O}_7$ due to the significant role of terms with S_i^+ and S_j^- in \mathcal{H}_{ex} ²³. These terms are sufficiently large to drive a transition to canted ferromagnetic order (C-FM) in powder samples³⁷¹⁷ and stoichiometric single crystals²⁵¹⁷ at $T_{\text{CFM}} = 275 \text{ mK}$. Meanwhile, the paramagnetic state above T_{CFM} shows hallmarks of strong correlations and fluctuations such as an anomalous increase of T_{CFM} with $|H| > 0^{25}$, pinch-points in diffuse neutron scattering²⁴, and strongly broadened, possibly gapless, inelastic neutron scattering spectra³²³⁷. Significant spin-entropy is released up to $T = 3 \text{ K}^{17}$, the characteristic energy scale of the dominant spin-spin interaction²⁶.

Summary of experimental observations. The key features of our thermal transport experiments, using a standard geometry with three semiconducting thermometers and a chip heater attached to a thin $\langle 111 \rangle$ plate with $\mathbf{J}_Q // \langle 1\bar{1}0 \rangle^{18}$, are summarized in Fig. 1 (c-f): Very large $\kappa_{xy}/T > 0$ (entropy factor removed) is observed at $T < 3 \text{ K}$ in the vicinity of zero field, until the signal is suppressed just below the phase transition to the C-FM state. Meanwhile, $\kappa_{xy}/T < 0$ is a characteristic feature of the field-aligned ferromagnetic state (FA-FM, $H > 1 \text{ T}$) at the lowest T . At very large fields, the thermal Hall signal is suppressed to zero, consistent with a large gap of magnetic excitations induced by the Zeeman effect.

Our sample was taken from the same batch as the one used for specific heat $c_P(T)$ measurements in Ref.²⁵. At T_{CFM} , where a sharp spike was observed in $c_P(T)$ (Ref.¹⁷²⁵ and Fig. 4, inset), we found a kink in $\kappa_{xx}(T)$ in zero field (Fig. 2 (b)). However, we also found that our $T_{\text{CFM}} = 0.265 \text{ K}$ was slightly reduced as compared to the previous report

($T_{\text{CFM}}^{\text{Arpino}} = 0.275 \text{ K}$)¹⁷¹⁸. This may be associated with a mild deterioration of the sample quality during the preparation process¹⁸.

Discussion of phonon skew scattering. Recently, κ_{xy} in rare earth pyrochlore titanates has been discussed not only from the point of view of the intrinsic (Berry phase) theory of Eq. 1, but also using an extrinsic scattering mechanism (phonon skew scattering)³²⁷. In the present work, we demonstrate that κ_{xy}/T in $\text{Yb}_2\text{Ti}_2\text{O}_7$ exhibits highly nonlinear behavior as a function of H and T , qualitatively at odds with the extrinsic scenario. We observed vanishing κ_{xy} when M approaches saturation, suppression of κ_{xy}/T around the ordering temperature, and even a sign change at intermediate H and low T .

A comparison of $\kappa_{xx}(T)$ for three rare earth titanates $R_2\text{Ti}_2\text{O}_7$ (R : rare earth) sheds further light on the phonon scattering behavior: (i) Non-magnetic $R = \text{Y}$ has negligible κ_{xy} ¹³ and has the largest κ_{xx} at low T . This corresponds to a large phonon mean-free path in the absence of resonant scattering from magnetic rare earth sites²⁸. (ii) κ_{xx} is strongly suppressed in $R = \text{Tb}$ with non-Kramers ion Tb^{3+} due to coupling of the ground state quasi-doublet to lattice vibrations. Experimentally, the observation of a hybrid magnetoelastic excitation in inelastic neutron scattering²⁹ is perhaps the clearest evidence of strong spin-lattice coupling in $R = \text{Tb}$, resulting in a very short phonon mean free path $\sim 1 \mu\text{m}$ ²⁸. (iii) In contrast, Yb^{3+} is a Kramers ion, i.e. spin-phonon coupling cannot lift the degeneracy of the ground state doublet and we expect phonon skew scattering to be suppressed. Although κ_{xx} of $R = \text{Yb}$ lies in an intermediate regime (Fig. 2 (a)), its κ_{xy}/T and thermal Hall angle $|\kappa_{xy}|/\kappa_{xx}$ are even larger than those of $R = \text{Tb}$ ¹⁸. We conclude that the thermal Hall signal reported in this manuscript is inconsistent with the phonon skew scattering mechanism³.

Field-aligned ferromagnetic state. In the FA-FM state, the presence of sharp magnon quasiparticle modes has been established convincingly in inelastic neutron scattering and THz experiments³⁰³¹³². This is the regime where $\kappa_{xy} < 0$ was observed in our experiment at $1 \text{ T} < H < 3 \text{ T}$ (Fig. 3). Using the experimental magnon spectra, repeated attempts have been undertaken to determine the coupling constants in \mathcal{H}_{ex} . For example, the seminal work by Ross *et al.* reported negligible dipolar interactions and dominant spin-ice (Ising-like) correlations $\sim J_{zz}S_i^zS_j^z$ in \mathcal{H}_{ex} ³⁰. Meanwhile, fluctuation terms $\sim S_i^+S_j^-$, $\sim S_i^+S_j^+$, $\sim S_i^zS_j^+$, etc. were also found to be significant³⁰. A successive experimental study, exploring a wide range of reciprocal space, reported Hamiltonian parameters at odds with the initial work³²; ambiguities thus remain concerning the reliability of such fitting schemes.

Our thermal transport study provides a highly desirable, independent check on these neutron scattering experiments, clarifying firstly that there are no additional lower-energy magnon bands with finite Berry curvature at $H > 1$ T. Secondly, although this is beyond the scope of the present paper, the κ_{xy} data can be modeled quantitatively when assuming a given set of Hamiltonian parameters. Thirdly, some key parameters describing the magnon spectrum in the FA-FM state can be extracted by treating κ_{xy} phenomenologically. When a Zeeman gap is opened in $H \neq 0$, the T -dependence of κ_{xy} is dominated by changes in the number density of heat carrying excitations and we crudely simplify Eq. 1 to

$$\begin{aligned}\kappa_{xy}/T &= (\bar{\kappa}_{xy}/T) \cdot \exp(-\beta(\Delta_{A,\text{HF}} + \Delta_{Z,\text{HF}})) \\ &= (\kappa_{xy}^{(0)}/T) \cdot \exp(-\beta\Delta_{Z,\text{HF}})\end{aligned}\quad (2)$$

The total spin gap is a combination of H -dependent Zeeman gap $\Delta_{Z,\text{HF}} = (g_{\text{eff}}/2)\mu_B H$ and H -independent anisotropy gap $\Delta_{A,\text{HF}}$. Here, μ_B is the Bohr magneton and $\beta = (k_B T)^{-1}$ with Boltzmann constant k_B . We have introduced an averaged, effective g -factor defined for pseudospin-1/2, but the reader should be aware that neutron scattering experiments have reported significant anisotropy of g in $\text{Yb}_2\text{Ti}_2\text{O}_7$ ^{32,30}. The reduced $(\kappa_{xy}^{(0)}/T)$ may contain additional, subdominant power-law T -dependence⁹.

We test Eq. 2 using a scaling analysis in the FA-FM state as shown in Fig. 3 (b). All the curves of $\ln |\kappa_{xy}/T|$ are found to collapse onto a universal line as a function of $\beta\Delta_{Z,\text{HF}} \sim H/T$, if a H -independent term $\sim \beta\Delta_{A,\text{HF}}$ is subtracted. This yields $g_{\text{eff}} = 2.8$. Fitting the H -independent term $\ln |\kappa_{xy}^{(0)}/T|$ as a function of T , we also estimate the anisotropy gap in the FA-FM state: $\Delta_{A,\text{HF}} = 78 \mu\text{eV}$ (Fig. 3 (c)). Note that $\Delta_{A,\text{HF}}$ in the FA-FM state is distinct from excitation gap of the C-FM state at low H .

Thermal Hall effect in the correlated paramagnetic state. As alluded to earlier in the text, the fluctuating correlated-paramagnetic state of $\text{Yb}_2\text{Ti}_2\text{O}_7$ hosts a very large *positive* κ_{xy} signal just above T_{CFM} . We study the linear response in this regime through the low- H slope of the thermal Hall conductivity $[\kappa_{xy}/(TH)]_0 = [\kappa_{xy}/(TH)]_{H \rightarrow 0}$ (Fig. 4). The onset of finite $[\kappa_{xy}/(TH)]_0$ occurs just below $T = 3$ K, in good agreement with a hump in $c_P(T)$ around the same T ³⁵. As T is lowered further, $[\kappa_{xy}/(TH)]_0$ increases sharply below 0.5 K, reaches a maximum around 0.35 K, and then finally starts to decrease as T_{CFM} is approached from above and transgressed (Fig. 4). We compare with $c_P(T)$ for a sample from the same batch (inset of Fig. 4, adapted from Ref.¹⁷). The presence of a maximum in $[\kappa_{xy}/(TH)]_0$

at $T = 0.4$ K strongly suggests that the spin gap of the PM state should be smaller than $40 \mu\text{eV}$.

A regime of enhanced $[\kappa_{xy}/(TH)]_0$ just above T_{CFM} as reported here was foreshadowed in a combined study of elastic neutron scattering and bulk techniques by Scheie *et al.*²⁵. These authors reported that small $\mathbf{H} // \langle 111 \rangle$ can suppress fluctuations in the correlated-paramagnetic state, increasing T_{CFM} and resulting in an unconventional lobe-shaped phase diagram (Fig. 1 (f), (black symbols))²⁵. In our data, the largest $[\kappa_{xy}/(TH)]_0$ is observed in the fluctuation region identified by Ref.²⁵. In fact, the positive thermal Hall signal takes on record values as compared to κ_{xx} . We report the maximum value of the Hall angle $|\kappa_{xy}^{\text{max}}|/\kappa_{xx}$ as a function of T in Fig. 4 (b). The peak magnitude of nearly 2% is about three times larger than any previously reported signal³⁶.

Discussion and conclusion. Previously, some attempts have been made in systems with long-range order to model the thermal Hall signal in the correlated-paramagnetic regime using Schwinger-boson linearization of the Hamiltonian and Eq. 1. In the layered Kagome ferromagnet Cu(1,3-bdc), sizable κ_{xy} observed above the onset of long-range order¹⁰ was explained in this framework¹¹. A weaker, H -linear signal appears in frustrated Kagome systems with antiferromagnetic nearest-neighbor exchange and strongly suppressed, yet non-zero, T_N ¹⁴¹⁵.

For $\text{Yb}_2\text{Ti}_2\text{O}_7$ we speculate that the approximation of non-interacting particles underlying Eq. 1 may break down completely in the correlated-paramagnetic regime, especially around T_{CFM} . This hypothesis is supported by the experimental observation of a very broad inelastic scattering continuum in $\text{Yb}_2\text{Ti}_2\text{O}_7$ at low H , even below T_{CFM} ³²³⁷³³, which may be connected to strongly interacting two-magnon states³². In this scenario, a quantitative comparison of our low- H κ_{xy} data to theory requires a generalization of the standard framework of Refs.⁵⁶ (Eq. 1) to the case of strongly interacting magnon states³⁸. Alternatively, Eq. 1 may retain its validity if the broad neutron scattering spectrum is related to quasiparticle fractionalization³⁸³⁹⁴⁰. In either case, the experiment demonstrates that gigantic thermal Hall responses can be generated from magnetic excitations in the absence of long-range order. We expect that our work will further the ongoing search³⁶ for giant κ_{xy} and related spin-Hall and spin-Nernst effects in the solid state.

Acknowledgments. We thank R.J. Cava and J. Krizan for initial attempts at float zoning crystal growth for $\text{Yb}_2\text{Ti}_2\text{O}_7$. We also acknowledge stimulating discussions with S. On-

oda. C. Pfeleiderer and S. Säubert kindly made their low- T magnetization data from Ref.²⁵ available to us. The research at Princeton was supported by the Department of Energy (DE-SC0017863), the Gordon and Betty Moore Foundation’s EPiQS initiative through Grants GBMF4539, and the U.S. National Science Foundation (Grant DMR 1420541). The work at the Institute for Quantum Matter, an Energy Frontier Research Center, was supported by the U.S. Department of Energy, Office of Science, Office of Basic Energy Sciences under Award Number DE-SC0019331.

* maximilian.hirschberger@riken.jp; Current address: RIKEN Center for Emergent Matter Science (CEMS), Wako 351-0198, Japan

1. J. M. Ziman, *Principles of the Theory of Solids*, 2nd Edition (1964)
2. The externally applied field is reported in units of Tesla (factor μ_0 was omitted). See Supplementary Information.
3. C. Strohm, G. L. J. A. Rikken, and P. Wyder, *Phenomenological Evidence for the Phonon Hall Effect*, Physical Review Letters **95**, 155901 (2005); C. Strohm, PhD thesis, Universität Konstanz (2003)
4. H. Katsura, N. Nagaosa, and P. A. Lee, *Theory of the Thermal Hall Effect in Quantum Magnets*, Physical Review Letters **104**, 066403 (2010)
5. R. Matsumoto and S. Murakami, *Theoretical Prediction of a Rotating Magnon Wave Packet in Ferromagnets*, Physical Review Letters **106**, 197202 (2011)
6. S. Murakami and A. Okamoto, *Thermal Hall Effect of Magnons*, Journal of the Physical Society of Japan **86**, 011010 (2017)
7. W.-L. Lee *et al.*, *Dissipationless Anomalous Hall Current in the Ferromagnetic Spinel $\text{CuCr}_2\text{Se}_{4-x}\text{Br}_x$* , Science **303**, 1647 (2004)
8. N. Nagaosa, J. Sinova, S. Onoda, A. H. MacDonald, and N. P. Ong, *Anomalous Hall effect*, Rev. Mod. Phys. **82**, 1539 (2010)
9. Y. Onose *et al.*, *Observation of the Magnon Hall Effect*, Science **329**, 297 (2010); T. Ideue *et al.*, *Effect of lattice geometry on magnon Hall effect in ferromagnetic insulators*, Physical Review B **85**, 134411 (2012)
10. M. Hirschberger *et al.*, *Thermal Hall effect of spin excitations in a kagome magnet*, Physical

- Review Letters **115**, 106603 (2015)
11. H. Lee, J. H. Han, and P. A. Lee, *Thermal Hall effect of spins in a paramagnet*, Physical Review B **91**, 125413 (2015)
 12. J. Romhányi, K. Penc, and R. Ganesh, *Hall effect of triplons in a dimerized quantum magnet*, Nature Communications **6**:6805 (2015)
 13. M. Hirschberger *et al.*, *Large thermal Hall conductivity of neutral spin excitations in a frustrated quantum magnet*, Science **348**, 106 (2015)
 14. D. Watanabe *et al.*, *Emergence of nontrivial magnetic excitations in a spin-liquid state of kagomé volborthite*, Proceedings of the National Academy of Sciences **113** 8653-8657 (2016)
 15. H. Doki *et al.*, *Spin Thermal Hall Conductivity of a Kagome Antiferromagnet*, Physical Review Letters **121**, 097203 (2018)
 16. Y. Kasahara *et al.*, *Majorana quantization and half-integer thermal quantum Hall effect in a Kitaev spin liquid*, Nature **559**, 227 (2018)
 17. K. E. Arpino *et al.*, *Impact of stoichiometry of $Yb_2Ti_2O_7$ on its physical properties*, Physical Review B **95**, 094407 (2017)
 18. Supplementary Information
 19. J. Gaudet *et al.*, *Neutron spectroscopic study of crystalline electric field excitations in stoichiometric and lightly stuffed $Yb_2Ti_2O_7$* , Physical Review B **92**, 134420 (2015)
 20. P. W. Anderson, *Ordering and Antiferromagnetism in Ferrites*, Physical Review **102**, 1008 (1956)
 21. A. P. Ramirez *et al.*, *Zero-point entropy in 'spin ice'*, Nature **339**, 333-335 (1999)
 22. C. Castelnovo, R. Moessner, and S. L. Sondhi, *Magnetic monopoles in spin ice*, Nature **451**, 42 (2008)
 23. M. J. P. Gingras and P. A. McClarty, *Quantum spin ice: a search for gapless quantum spin liquids in pyrochlore magnets*, Reports on Progress in Physics **77**, 056501 (2014)
 24. L.-J. Chang *et al.*, *Higgs transition from a magnetic Coulomb liquid to a ferromagnet in $Yb_2Ti_2O_7$* . Nature Communications **3**:992 (2012)
 25. A. Scheie *et al.*, *Reentrant Phase Diagram of $Yb_2Ti_2O_7$ in a $\langle 111 \rangle$ Magnetic Field*, Physical Review Letters **119**, 127201 (2017)
 26. A. M. Hallas, J. Gaudet, and B. D. Gaulin, *Experimental Insights into Ground-State Selection of Quantum XY Pyrochlores*, Annual Review of Condensed Matter Physics **9**, 105 (2017)

27. Y. Hirokane *et al.*, *Phononic thermal Hall effect in diluted terbium oxides*, Physical Review B **99**, 134419 (2019)
28. Q. J. Li *et al.*, *Phonon-glass-like behavior of magnetic origin in single-crystal $Tb_2Ti_2O_7$* , Physical Review B **87**, 214408 (2013)
29. T. Fennell *et al.*, *Magnetoelastic Excitations in the Pyrochlore Spin Liquid $Tb_2Ti_2O_7$* , Physical Review Letters **112**, 017203 (2014)
30. K. A. Ross *et al.*, *Quantum Excitations in Quantum Spin Ice*, Physical Review X **1**, 021002 (2011)
31. L. Pan *et al.*, *Low-energy electrodynamics of novel spin excitations in the quantum spin ice $Yb_2Ti_2O_7$* , Nature Communications **5**:4970 (2014)
32. J. D. Thompson *et al.*, *Quasiparticle Breakdown and Spin Hamiltonian of the Frustrated Quantum Pyrochlore $Yb_2Ti_2O_7$ in Magnetic Field*, Physical Review Letters **119**, 057203 (2017)
33. S. Onoda, private communications
34. Y. Tokiwa *et al.*, *Possible observation of highly itinerant quantum magnetic monopoles in the frustrated pyrochlore $Yb_2Ti_2O_7$* , Nature Communications **7**, 10807 (2016)
35. J. A. Hodges *et al.*, *First-Order Transition in the Spin Dynamics of Geometrically Frustrated $Yb_2Ti_2O_7$* , Physical Review Letters **88**, 077204 (2002)
36. T. Ideue *et al.*, *Giant thermal Hall effect in multiferroics*, Nature Materials **16**, 797802 (2017)
37. V. Pecanha-Antonio *et al.*, *Magnetic excitations in the ground state of $Yb_2Ti_2O_7$* , Physical Review B **96**, 214415 (2017)
38. J. G. Rau, R. Moessner, and P. A. McClarty, *Magnon interactions in the frustrated pyrochlore ferromagnet $Yb_2Ti_2O_7$* , arxiv:1903.05098 (2019)
39. T.-H. Han *et al.*, *Fractionalized excitations in the spin-liquid state of a kagome-lattice antiferromagnet*, Nature **492**, 406 (2012)
40. A. Banerjee *et al.*, *Proximate Kitaev quantum spin liquid behaviour in a honeycomb magnet*, Nature Materials **15**, 733 (2016)

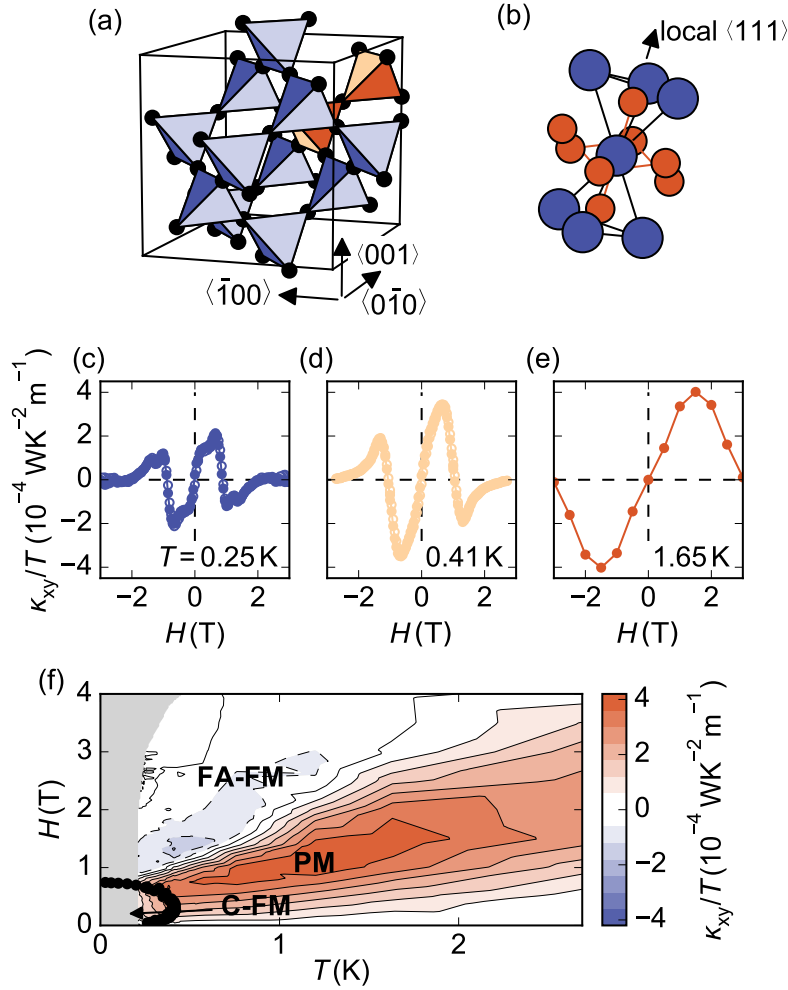


FIG. 1. (color online). (a) Pyrochlore crystal structure of $\text{Yb}_2\text{Ti}_2\text{O}_7$. Only the rare-earth sublattice is shown (black dots), forming a network of corner-sharing tetrahedra. A pair of rare-earth tetrahedra is highlighted in red color. Crystallographic directions are indicated by arrows. (b) The crystal fields at each rare earth site (blue) are dominated by the surrounding oxygen ions (red). Ti^{4+} ions not shown. Local $\langle 111 \rangle$ direction for central rare earth ion is marked by an arrow. (c-e) Field dependence of κ_{xy}/T at various T , with $\mathbf{H} \parallel \langle 111 \rangle$, and heat current $\mathbf{J}_Q \parallel \langle 110 \rangle$. (f) Contour plot of thermal Hall conductivity κ_{xy}/T . Black circles mark the phase transition between canted ferromagnetic (C-FM) order and the paramagnetic (PM) state (from Ref.²⁵). FA-FM is the field-aligned ferromagnetic state.

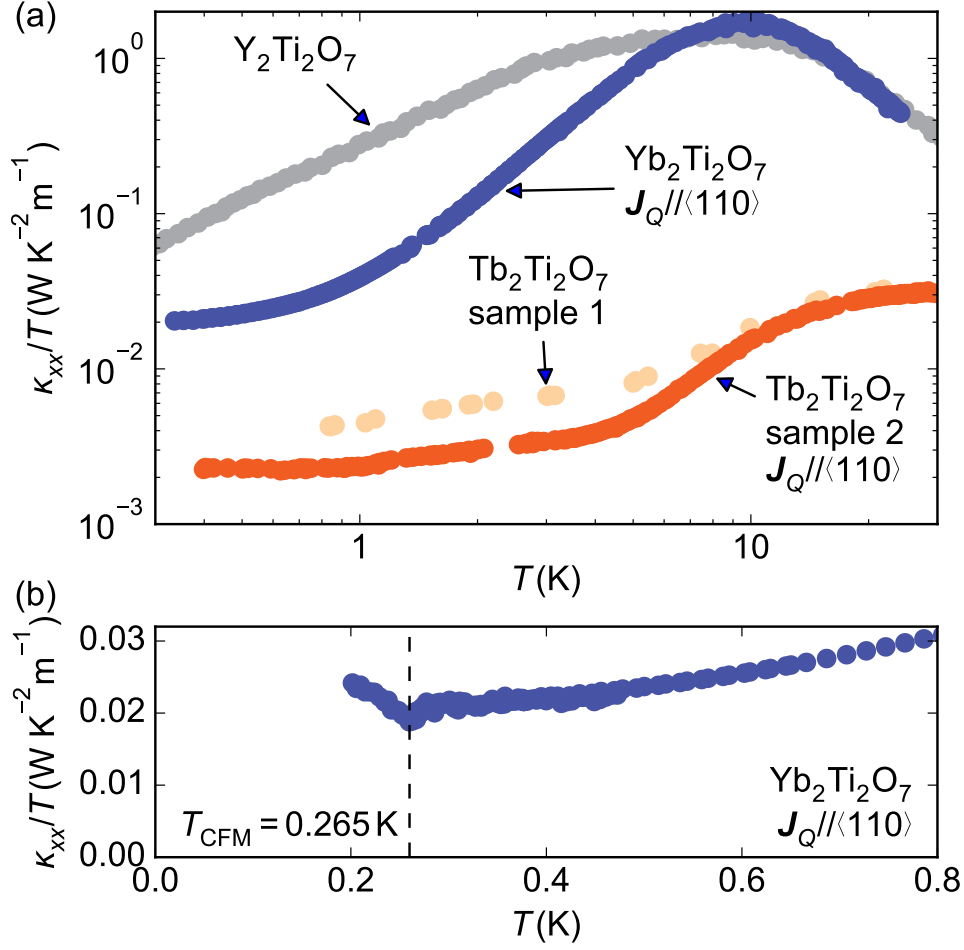


FIG. 2. (color online). (a) Comparison of zero-field thermal conductivity κ_{xx} for various $R_2\text{Ti}_2\text{O}_7$ compounds. At high $T \sim 20 \text{ K}$, the large maximum of κ_{xx} in $R = \text{Yb}$ indicates excellent sample quality. Phonon scattering at low T is strongest in $R = \text{Tb}$ (from Ref.¹³), and weakest in non-magnetic $R = \text{Y}$ (from Ref.²⁸). (b) Low- T κ_{xx}/T for $R = \text{Yb}$, showing a kink in the curve at the phase transition to long-range order (black dashed line).

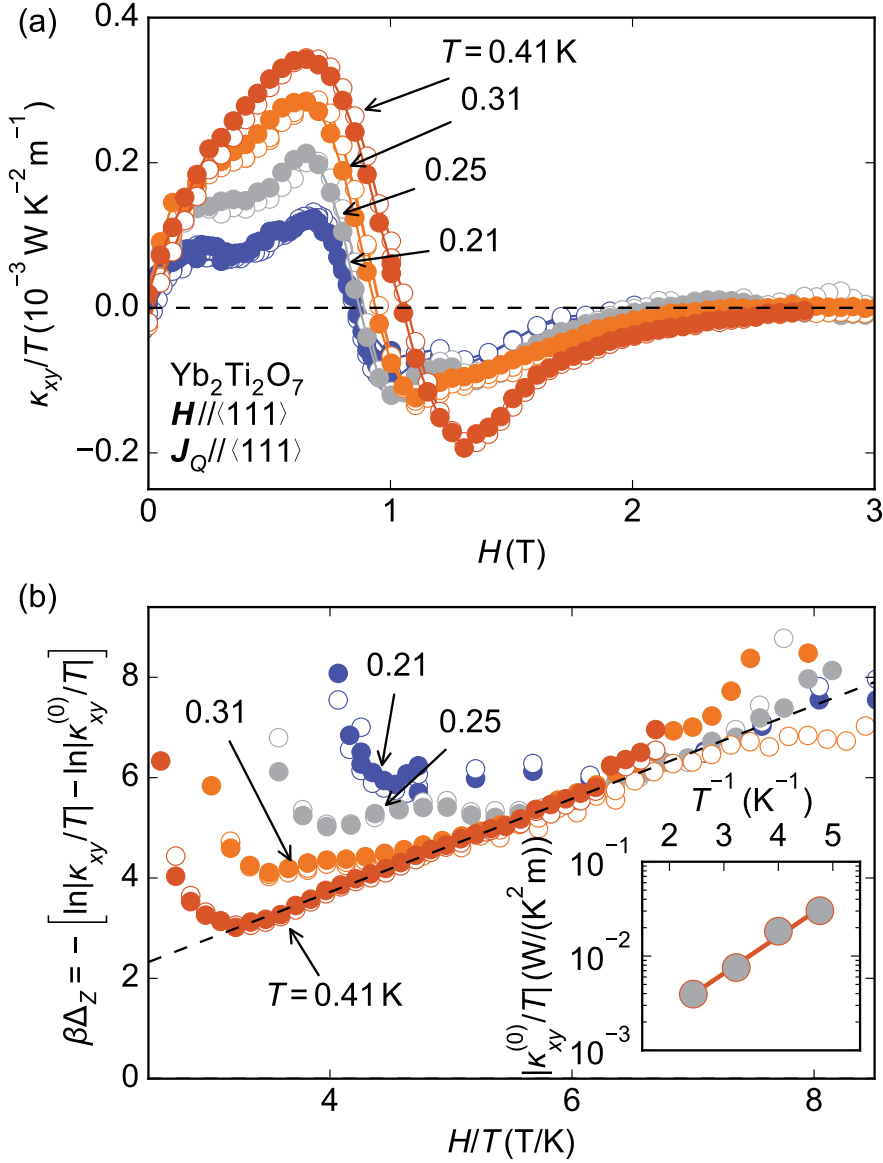


FIG. 3. (color online). Scaling analysis of κ_{xy}/T for $\text{Yb}_2\text{Ti}_2\text{O}_7$ in the field-aligned ferromagnetic state. (a) Raw data of the thermal Hall conductivity κ_{xy}/T ; we focus on the negative signal observed for $\mu_0 H > 1 \text{ T}$. (b) According to Eq. 2, linear $\ln|\kappa_{xy}/T| \sim H/T$ is expected. A fit to the $T = 0.41 \text{ K}$ data (dashed line) yields the effective g -factor (see text). The inset of (b) shows exponential T dependence of the field-independent term $\kappa_{xy}^{(0)}/T$ from Eq. (2), from which the high-field anisotropy gap $\Delta_{\text{A,HF}} = 78 \mu\text{eV}$ was extracted by a fit (red line).

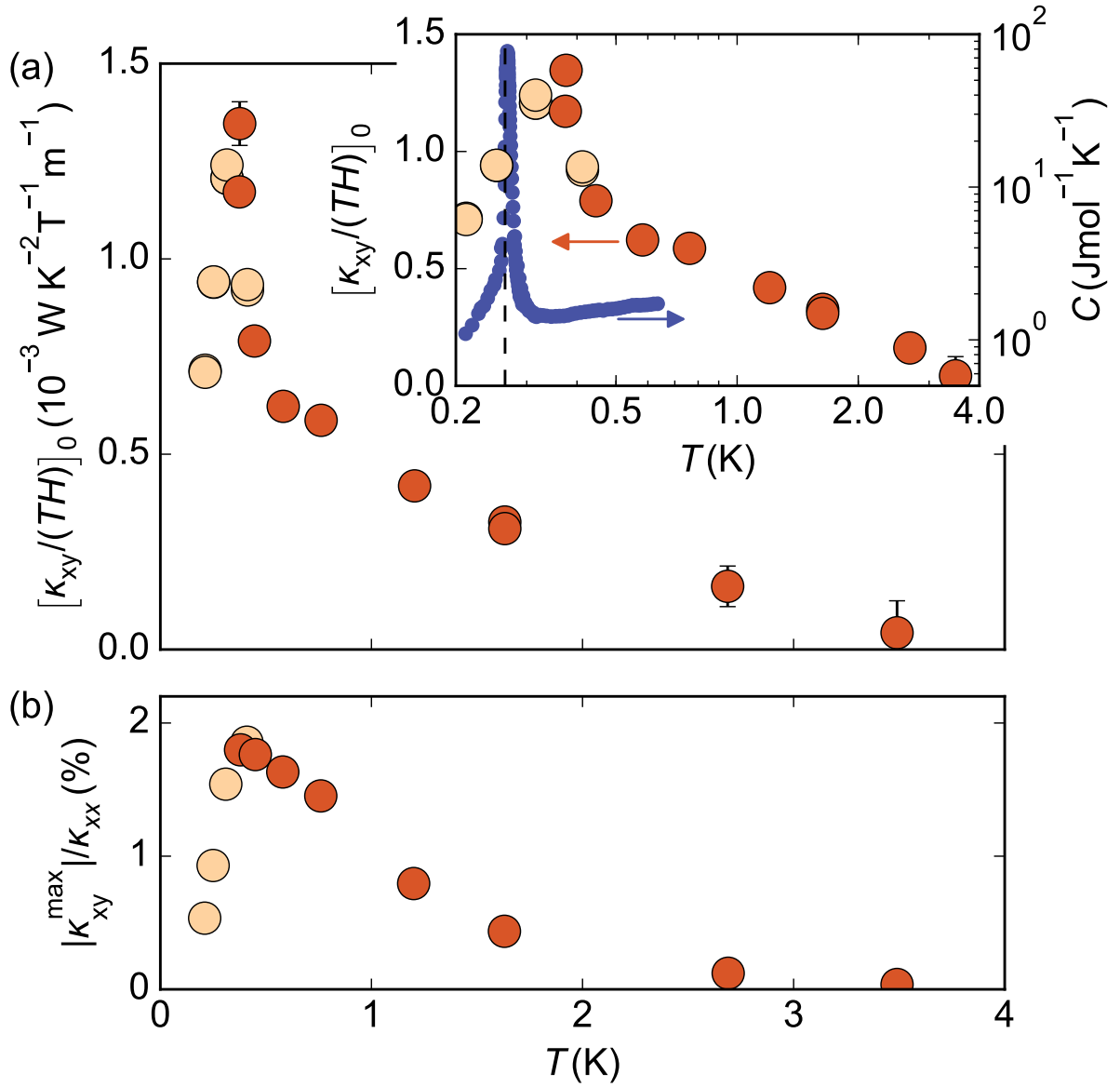


FIG. 4. (color online). (a) The initial slope $[\kappa_{xy}/(TH)]_0$ of the thermal Hall conductivity in $\text{Yb}_2\text{Ti}_2\text{O}_7$. Inset: On a logarithmic T -scale, the regime of largest $[\kappa_{xy}/(TH)]_0$ is clearly identified to be above the ordering transition (dashed black line). The ordering temperature T_{CFM} was defined through the specific heat $c_P(T)$ from Ref.¹⁷ (blue, right axis). T_{CFM} of the thermal transport sample is ~ 10 mK lower than in the case of $c_P(T)$ (c.f. main text). (b) Peak thermal Hall angle obtained by choosing the maximum value of each $|\kappa_{xy}|/\kappa_{xx}$ isotherm. Yellow symbols represent data recorded in a dilution refrigerator, while red data points were taken using a He-3 insert.